Asymmetric jet clustering in deep-inelastic scattering

M. Arratia,[1,2,*] Y. Makris,[3,†] F. Ringer,[4,‡] and N. Sato[5,§]

[1] *Physics Department, University of California, Riverside, CA 92521, USA*
[2] *Thomas Jefferson National Accelerator Facility, Newport News, VA 23606, USA*
[3] *INFN Sezione di Pavia, via Bassi 6, I-27100 Pavia, Italy*
[4] *Nuclear Science Division, Lawrence Berkeley National Laboratory, Berkeley, California 94720, USA*
[5] *Theory Center, Jefferson Laboratory, Newport News, Virginia 23606, USA*

(Dated: June 15, 2020)

We propose a new class of jet algorithms for deep-inelastic Scattering (DIS) that accounts for the forward-backward asymmetry in the Breit frame, which we call Centauro. The Centauro algorithm is longitudinally-invariant and properly clusters jets resulting from the DIS Born configuration, which makes it suited for novel studies of transverse-momentum-dependent observables. Furthermore, we show that spherically-invariant algorithms in the Breit frame give access to the low energy spectrum of jets in the current fragmentation region. We propose studies in unpolarized, polarized, and nuclear DIS at the future Electron-Ion Collider.

Introduction. Understanding the structure of nucleons and nuclei in terms of quark and gluon degrees of freedom is one of the main goals of modern nuclear physics. Jet production in deep inelastic scattering (DIS) provides an excellent tool for this endeavour. The future Electron-Ion Collider (EIC) [1] will produce the first jets in polarized and nuclear DIS, which will enable a rich jet physics program, as highlighted recently in refs. [2–31].

The HERA jet measurements targeted higher-order processes to constrain the strong-coupling constant and the gluon parton distribution function (PDF) [32]. In these measurements the Born kinematics, $\gamma^* q \to q$, was suppressed by requiring large transverse momentum in the Breit frame [33]. Recently, jet produced close to the Born kinematics was postulated as a probe for the transverse-momentum dependent (TMD) distribution of quarks within nucleons [34–36]. Jet measurements allow for a direct access to TMD PDFs as the final state jet can be calculated perturbatively and does not require a nonperturbative TMD fragmentation function. Hadronization corrections can be minimized with grooming or recoil-free axis.

The factorization of the TMD sensitive cross section in the Breit frame involves the same universal soft and unsubtracted TMD functions as in Drell-Yan and $e^+e^- \to$ dihadron/dijet processes. However, jet algorithms commonly used in DIS are longitudinally-invariant but fail to cluster jets close to the Born kinematics in the Breit frame since they use distance measures in rapidity-azimuth plane and thus cannot form a jet enclosing the beam directions. Therefore, measurements of jets close to Born kinematics require a new longitudinally invariant jet algorithm optimized for the Breit frame, which we introduce in this letter.In addition, we consider the use of spherically-invariant algorithms to study the energy spectrum of jets as they separate the current and target fragmentation regions even for soft jets.

Notation and DIS kinematics. In the Breit frame, the virtual photon momentum is:

$$q^\mu = \frac{Q}{2}(\bar{n}^\mu - n^\mu) = Q(0,0,0,-1)\,, \tag{1}$$

where $n^\mu \equiv (1,0,0,+1)$ and $\bar{n}^\mu \equiv (1,0,0,-1)$. The proton momentum (up to mass corrections) is:

$$P^\mu \simeq Q/(2x_B)n^\mu = Q/(2x_B)(1,0,0,+1)\,, \tag{2}$$

with Bjorken $x_B \equiv Q^2/(2\,q\cdot P)$. At Born level, a quark is struck by the virtual photon and recoils in the opposite direction of the proton with momentum ($x \simeq x_B$):

$$p_q^\mu = xP^\mu + q^\mu \simeq (Q/2)\bar{n}^\mu\,. \tag{3}$$

The fragmentation of the struck-quark yields a jet with similar momentum pointing in the Breit frame beam direction. The algorithms we introduce below are designed to capture this jet. We measure the inclusive jet energy spectrum in terms of the scaling variable $z_{\rm jet}$:

$$z_{\rm jet} = \frac{P\cdot p_{\rm jet}}{P\cdot q}\,. \tag{4}$$

At leading logarithmic accuracy $z_{\rm jet}$ corresponds to the fraction of the struck quark momentum carried by the jet and in the Breit frame we have, $z_{\rm jet} \simeq p_{\rm jet}^-/Q$.

New jet algorithms for DIS. Longitudinally invariant algorithms, such as the k_T-type algorithms [37],

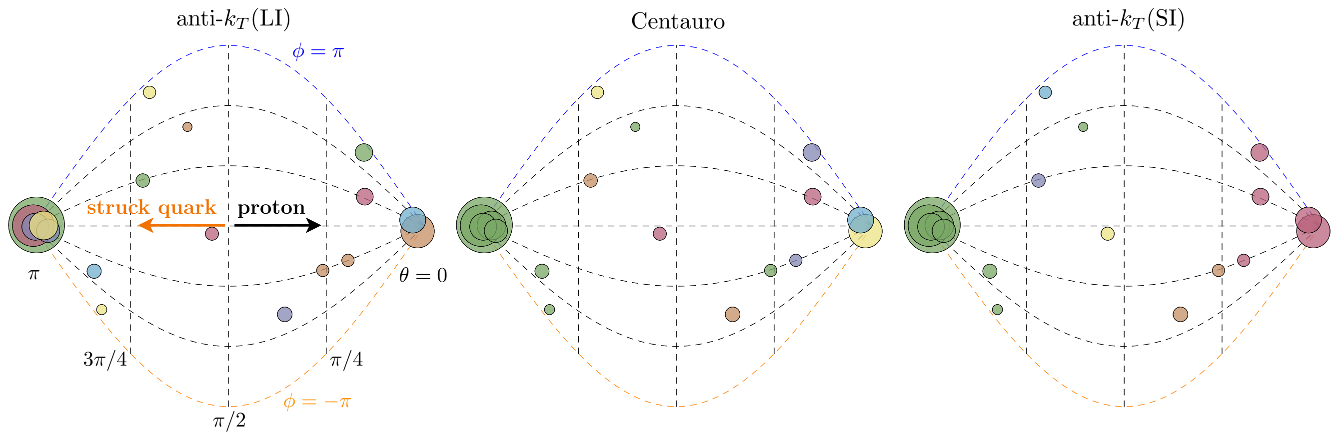

Figure 1. Jet clustering in the Breit frame using the longitudinally-invariant anti-k_T(LI), Centauro, and spherically-invariant anti-k_T(SI) algorithms in a DIS event simulated with PYTHIA 8. Each particle is illustrated as a disk with area proportional to its energy. The direction of the momentum of each particle is given by its position on the unfolded sphere about the hard-scattering vertex, where vertical dashed lines correspond to constant θ and curved lines to constant ϕ. All particles clustered into a specific jet are colored the same.

cluster particles in terms of their distance in the rapidity-azimuth ($y-\phi$) plane and thus cannot form a jet enclosing the anti-beam direction $\bar{n}^\mu$. The distance measure used for those k_T-type algorithms is

$$d_{ij} = \min(p_{Ti}^{2p}, p_{Tj}^{2p})\Delta R_{ij}^2/R^2 \,, \qquad d_{iB} = p_{Ti}^{2p} \tag{5}$$

where $\Delta R_{ij} = (y_i - y_j)^2 + (\phi_i - \phi_j)^2$. Here d_{ij} is the distance between two particles in the event and d_{iB} is the beam distance.

One way to bypass this problem is to use spherically-invariant algorithms such as the anti-k_T jet algorithm for e^+e^- collisions [37]. The distance measure for these algorithms is

$$d_{ij} = \min(E_i^{2p}, E_j^{2p})\frac{1-c_{ij}}{1-c_R} \,, \qquad d_{iB} = E_i^{2p} \,, \tag{6}$$

where $c_{ij} = \cos\theta_{ij}$ and $c_R = \cos R$ which we study below in more detail. These type of algorithms lack the longitudinal invariance that permits to connect the results to frames linked to the Breit frame via a boost in the $\hat{z}$ direction, which form a class with crucial features for jet clustering in DIS [38]. For example, these are appropriate for multijet events where the parton kinematics is not constrained by x_B and Q^2, or to identify photo-production, pileup, and the beam remnant [39].

To solve this issue, we introduce a new hybrid jet algorithm that is longitudinally invariant along the Breit frame beam axis but yet captures the struck-quark jet. The use of spherically-invariant jet algorithms adapted to DIS was first proposed by Catani et al. [40]. More recently, Boronat et al [41] proposed a hybrid algorithm designed to suppress $\gamma\gamma$ background in e^+e^- colliders. [41]. In contrast, we suggest an asymmetric jet clustering algorithm, and suggest novel studies for spherically-invariant algorithms in DIS.

Starting with the distance measure of the generalized k_T algorithm for e^+e^- (eq. (6) for $p = 0$), we write the numerator in terms of the unit vectors along the directions of particles i and j,

$$1 - c_{ij} = 1 - \hat{n}_i \cdot \hat{n}_j = 1 - s_i s_j \cos\Delta\phi_{ij} - c_i c_j \,. \tag{7}$$

with $c_i = \cos\theta_i$ and $s_i = \sin\theta_i$. Expanding in the very backward limit (i.e. $\bar{\theta}_i \equiv \pi - \theta_i \ll 1$):

$$1 - c_{ij} \simeq \frac{1}{2}(\bar{\theta}_i - \bar{\theta}_j)^2 + \bar{\theta}_i\bar{\theta}_j(1 - \cos\Delta\phi_{ij}). \tag{8}$$

The new measure is found by making the replacements:

$$\bar{\theta}_i \to f_i = f(\bar{\eta}_i) \,, \qquad \bar{\eta}_i \equiv -\frac{2Q}{\bar{n}\cdot q}\frac{p_i^\perp}{n\cdot p_i} \,, \tag{9}$$

where the function f must satisfy: $f(x) = x + \mathcal{O}(x^2)$. In the Breit frame, the term $\bar{\eta}_i = 2p_i^\perp/(n\cdot p_i)$ introduces a backward-forward asymmetry. We introduce the following distance measure:

$$d_{ij} = (\Delta f_{ij})^2 + 2 f_i f_j (1 - \cos\Delta\phi_{ij})/R^2 \,, \quad d_{iB} = 1 \tag{10}$$

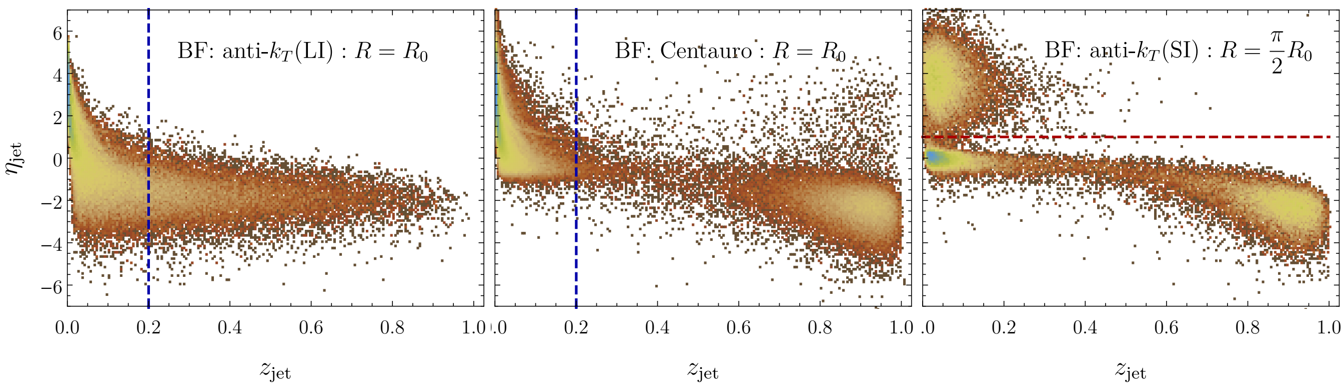

Figure 2. The distribution of jets in terms of pseudorapidity and momentum fraction. The left, center, and right panels correspond to jets identified with the anti-k_T(LI), Centauro, and anti-k_T(SI) algorithm, respectively. The dashed lines indicate the separation of jets in the current and target fragmentation region.

which defines a new class of algorithms, which we call Centauro algorithms. Two relevant choices[42] for the function f are:

$$f(x) = x\,, \qquad\qquad f(x) = \sinh^{-1}(x)\,. \qquad (11)$$

The Centauro algorithm is invariant along the $\hat{z}$ direction, but in the backward hemisphere it matches the spherically-invariant algorithms, see eq. (6). This feature is largely independent of the choice of f.

Simulation results and applications. Throughout this letter we use for our analysis events with $Q > 10$ GeV simulated in Pythia 8 [43] for electron (10 GeV) on proton (100 GeV) DIS [44]. We have excluded neutrinos and particles with $|\eta| > 4$ or $p_T < 200$ MeV in the laboratory frame.

Fig. 1 illustrates the anti-k_T(LI), Centauro, and anti-k_T(SI) jet clustering for an exemplary Pythia 8 event. The anti-k_T(LI) algorithm clusters the particles from the fragmentation of the struck-quark into four different jets[45]. In contrast, the anti-k_T(SI) and Centauro algorithms cluster all of these particles into a single jet with $z_{\rm jet} \sim 1$. The Centauro algorithm mimics the features of the anti-k_T(SI) in the backward direction and the anti-k_T(LI) in the forward direction.

Furthermore, with the use of Centauro and anti-k_T(SI) jets it is also possible to effectively eliminate the contribution from the target fragmentation region by either choosing the leading jet or by imposing a cut on $z_{\rm jet} \sim 0.2-0.7$ as shown in Fig. 2. This allows for direct studies of quark TMD sensitive observables such as the Sivers function. For the anti-k_T(SI) [46] algorithm, it is possible to choose a cut on $\eta_{\rm jet} < 1$ which can also separate current and target regions without a cutoff on $z_{\rm jet}$ (right panel of Fig. 2). This allows for studies of the full $z_{\rm jet}$ spectrum, which cannot be accessed with hadron measurements, for which the current and target regions are not well separated [47, 48]. For comparison we also show the result for the anti-k_T(LI) algorithm in the left panel of Fig. 2.

Fig. 3 shows the $z_{\rm jet}$ and $\eta_{\rm jet}$ distributions of inclusive jets as described above. While in the backward region ($\eta_{\rm jet} < 0$) the Centauro and anti-k_T(SI) algorithms result in a peak at large $z_{\rm jet} \sim 1$, the anti-k_T(LI) separates that jet into multiple less energetic ones which yields a $z_{\rm jet}$ peak at small values. In the same plots we also show the distributions for jets clustered in the laboratory frame using anti-k_T(LI), which is an alternative way to capture jets at Born kinematics [10, 49], and then the momenta of these jets is transformed to the Breit frame. In the backward region (struck-quark hemisphere) the jets found by this procedure roughly correspond to the jets found by the Centauro and anti-k_T(SI) algorithms in the Breit frame. This validates Centauro and anti-k_T(SI) jets and confirms the notion of the jet as a proxy for the struck-quark in any frame, although each algorithm will have different sensitivity to TMD physics and require different factorizations.

The two distinct peaks at $z_{\rm jet} \sim 1$ and $z_{\rm jet} \sim 0$ in Fig. 3 correspond to backward and mid rapidity jets. The intermediate $z_{\rm jet}$ region of the inclusive jet spectrum is described in terms of semi-inclusive jet functions and DGLAP evolution [50–53]. The large-$z_{\rm jet}$ jets probe the threshold region [54], whereas the small-$z_{\rm jet}$ region probes the soft fragmentation of jets. The latter region connects to soft fragmentation in e^+e^- collisions [55–59] and small-

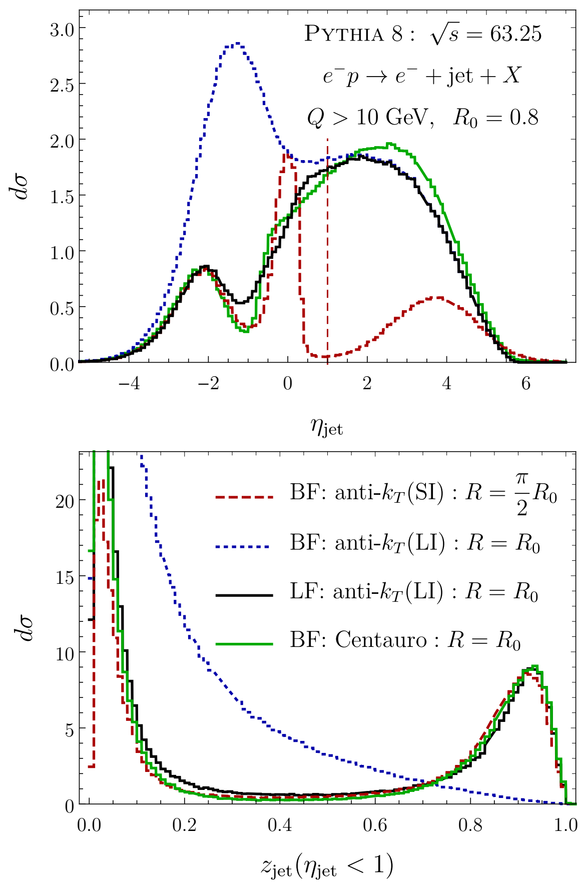

Figure 3. Pseudorapidity (top panel) and momentum fraction z_{jet} (bottom panel) of jets clustered with anti-k_T(LI), anti-k_T(LI) and Centauro algorithms in the Breit frame, as well as jets clustered in the laboratory frame with anti-k_T(LI).

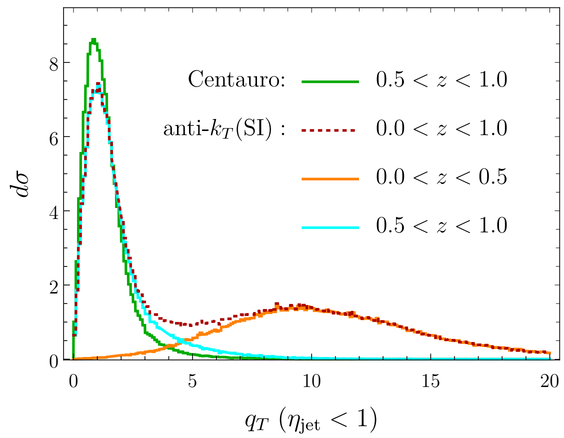

Figure 4. The $q_T = p_{\mathrm{jet}}^{\perp}/z_{\mathrm{jet}}$ spectrum for Centauro and anti-k_T(SI) jets with $\eta_{\mathrm{jet}} < 1.0$.

x physics [60–62].

We propose a measurement of z_{jet}, which has not been done before, and show projections for HERA and EIC kinematics in the Appendix. The high-z region correspond to jets with high-p_{T} in the laboratory frame that can be measured with high precision and with an accuracy limited by the jet energy scale uncertainty, which reached 1% at HERA [32]. The measurement of the small-z_{jet} region will be challenging because these jets have energies up to a few GeV in the laboratory frame, a region that can be limited by calorimeter noise and resolution. These issues could be bypassed by defining jets with charged particles only, which would require the inclusion of track-based jet function [63, 64] from the theory and low-thresholds from the experimental side.

We also propose to use Centauro jets to study the universal quark TMDs by measuring their $q_T = p_{\mathrm{jet}}^{\perp}/z_{\mathrm{jet}}$. The q_T spectrum for $z_{\mathrm{jet}} > 0.5$ is shown in Fig. 4. The spectrum is mainly concentrated in the region $q_T < Q_{\mathrm{min}}/4$ which is ideal for TMD phenomenology. In polarized DIS, this observable provides clean access to the quark Sivers function. We show projections for HERA and EIC kinematics in the Appendix. In the same figure we also show the distribution for anti-k_T(SI) jets for $z_{\mathrm{jet}} < 0.5$ and $0 < z_{\mathrm{jet}} < 1$. Note the latter is only possible since we can identify the target fragmentation by requiring $\eta_{\mathrm{jet}} < 1$. While for $z_{\mathrm{jet}} > 0.5$ we find similar result as the Centauro jets, for $z_{\mathrm{jet}} > 0.5$ we identify a contribution to the spectrum that peaks at $q_T \sim Q$, which arises from central rapidity jets. Novel theoretical techniques are necessary to describe this kinematic q_T region of jets.

The longitudinal invariance and ability to measure jets close to Born kinematics makes the Centauro algorithm an attractive option to: improve extractions of the strong coupling constant from the rates of n-jets [32]; for "tag-and-probe" studies of nuclei [49]; and to tag the background for gluon helicity and Sivers PDF studies at the EIC [65, 66].

Conclusions. We have proposed a new approach tailored to the study of energetic jets with low transverse momentum in DIS that relies on spherically-invariant algorithms and a new longitudinally-invariant algorithm that is asymmetric in the backward and forward directions, which we call Centauro. The Centauro algorithm enables novel studies of transverse-momentum-dependent observables in the Breit frame. Furthermore, we find that spherically symmetric k_T-type algorithms yield clean access to the soft jet fragmentation region, which reveals a new q_T regime, $q_T \sim Q$. The approach we advocate here is relevant for the studies of jet functions, quark TMD and spin observables, and to probe cold-nuclear matter. All these studies will be central for the jet physics program of the future Electron-Ion Collider.

Acknowledgement. We thank XXXX for insightful comments of our manuscript. M.A is partially supported through DOE Contract No. DE-AC05-06OR23177 under which JSA operates the Thomas Jefferson National Accelerator Facility

* miguel.arratia@ucr.edu
† yiannis.makris@pv.infn.it
‡ fmringer@lbl.gov
§ nsato@jlab.org

[1] A. Accardi *et al.*, Eur. Phys. J. **A52**, 268 (2016), 1212.1701.
[2] V. Guzey and M. Klasen, Eur. Phys. J. **C79**, 396 (2019), 1902.05126.
[3] R. Boughezal, F. Petriello, and H. Xing, Phys. Rev. **D98**, 054031 (2018), 1806.07311.
[4] M. Klasen and K. Kovařík, Phys. Rev. **D97**, 114013 (2018), 1803.10985.
[5] M. Klasen, K. Kovarik, and J. Potthoff, Phys. Rev. **D95**, 094013 (2017), 1703.02864.
[6] X. Chu, E.-C. Aschenauer, J.-H. Lee, and L. Zheng, Phys. Rev. **D96**, 074035 (2017), 1705.08831.
[7] A. Dumitru, V. Skokov, and T. Ullrich, Phys. Rev. **C99**, 015204 (2019), 1809.02615.
[8] P. Hinderer, M. Schlegel, and W. Vogelsang, Phys. Rev. **D96**, 014002 (2017), 1703.10872.
[9] P. Hinderer, M. Schlegel, and W. Vogelsang, Phys. Rev. **D92**, 014001 (2015), 1505.06415, [Erratum: Phys. Rev.D93,no.11,119903(2016)].
[10] X. Liu, F. Ringer, W. Vogelsang, and F. Yuan, Phys. Rev. Lett. **122**, 192003 (2019), 1812.08077.
[11] R. Kishore, A. Mukherjee, and S. Rajesh, (2019), 1908.03698.
[12] U. D'Alesio, F. Murgia, C. Pisano, and P. Taels, (2019), 1908.00446.
[13] L. Zheng, E. C. Aschenauer, J. H. Lee, B.-W. Xiao, and Z.-B. Yin, Phys. Rev. **D98**, 034011 (2018), 1805.05290.
[14] D. Boer, P. J. Mulders, C. Pisano, and J. Zhou, JHEP **08**, 001 (2016), 1605.07934.
[15] A. Dumitru, T. Lappi, and V. Skokov, Phys. Rev. Lett. **115**, 252301 (2015), 1508.04438.
[16] C. Pisano, D. Boer, S. J. Brodsky, M. G. A. Buffing, and P. J. Mulders, JHEP **10**, 024 (2013), 1307.3417.
[17] D. Boer, S. J. Brodsky, P. J. Mulders, and C. Pisano, Phys. Rev. Lett. **106**, 132001 (2011), 1011.4225.
[18] Z.-B. Kang, A. Metz, J.-W. Qiu, and J. Zhou, Phys. Rev. **D84**, 034046 (2011), 1106.3514.
[19] Y. Hatta, N. Mueller, T. Ueda, and F. Yuan, (2019), 1907.09491.
[20] H. Mäntysaari, N. Mueller, and B. Schenke, Phys. Rev. **D99**, 074004 (2019), 1902.05087.
[21] K. Roy and R. Venugopalan, (2019), 1911.04530.
[22] F. Salazar and B. Schenke, Phys. Rev. **D100**, 034007 (2019), 1905.03763.
[23] A. Dumitru and V. Skokov, Phys. Rev. **D94**, 014030 (2016), 1605.02739.
[24] Y. Hatta, B.-W. Xiao, and F. Yuan, Phys. Rev. Lett. **116**, 202301 (2016), 1601.01585.
[25] T. Altinoluk, N. Armesto, G. Beuf, and A. H. Rezaeian, Phys. Lett. **B758**, 373 (2016), 1511.07452.
[26] M. D. Sievert and I. Vitev, Phys. Rev. **D98**, 094010 (2018), 1807.03799.
[27] D. Kang, C. Lee, and I. W. Stewart, Phys. Rev. **D88**, 054004 (2013), 1303.6952.
[28] Z.-B. Kang, S. Mantry, and J.-W. Qiu, Phys. Rev. **D86**, 114011 (2012), 1204.5469.
[29] E.-C. Aschenauer, K. Lee, B. Page, and F. Ringer, Phys. Rev. D **101**, 054028 (2020), 1910.11460.
[30] Y.-Y. Zhang, G.-Y. Qin, and X.-N. Wang, Phys. Rev. D **100**, 074031 (2019), 1905.12699.
[31] Z.-B. Kang, K. Lee, and F. Zhao, (2020), 2005.02398.
[32] P. Newman and M. Wing, Rev. Mod. Phys. **86**, 1037 (2014), 1308.3368.
[33] K. H. Streng, T. F. Walsh, and P. M. Zerwas, Z. Phys. **C2**, 237 (1979).
[34] D. Gutierrez-Reyes, I. Scimemi, W. J. Waalewijn, and L. Zoppi, Phys. Rev. Lett. **121**, 162001 (2018), 1807.07573.
[35] D. Gutierrez-Reyes, I. Scimemi, W. J. Waalewijn, and L. Zoppi, JHEP **10**, 031 (2019), 1904.04259.
[36] D. Gutierrez-Reyes, Y. Makris, V. Vaidya, I. Scimemi, and L. Zoppi, JHEP **08**, 161 (2019), 1907.05896.
[37] M. Cacciari, G. P. Salam, and G. Soyez, Eur. Phys. J. **C72**, 1896 (2012), 1111.6097.
[38] B. Webber, J. Phys. G **19**, 1567 (1993).
[39] S. Catani, Y. L. Dokshitzer, M. Seymour, and B. Webber, Nucl. Phys. B **406**, 187 (1993).
[40] S. Catani, Y. L. Dokshitzer, and B. Webber, Phys. Lett. B **285**, 291 (1992).
[41] M. Boronat, J. Fuster, I. Garcia, E. Ros, and M. Vos, Phys. Lett. B **750**, 95 (2015), 1404.4294.
[42] Different choices can be optimized to match jets found by other algorithms, for example we found that jets found in the forward region are better matched to the jets clustered in the laboratory frame with the anti$-k_T$ algorithm.
[43] T. Sjostrand, S. Mrenna, and P. Z. Skands, Comput. Phys. Commun. **178**, 852 (2008), 0710.3820.
[44] In addition, we verified that our conclusions are the same when using the DIRE shower of ref. [67].
[45] Note that this cannot be corrected for by choosing a larger jet radius due to the exponential increase of the rapidity in the forward and backward region.
[46] Note that we include a factor of $\pi/2$ for the jet radius of

the anti-k_T(SI) algorithm to account for the difference in the denominator of the clustering metric in eq. (6) compared to eq. (5).

[47] M. Boglione *et al.*, Phys. Lett. B **766**, 245 (2017), 1611.10329.

[48] E. C. Aschenauer, I. Borsa, R. Sassot, and C. Van Hulse, Phys. Rev. **D99**, 094004 (2019), 1902.10663.

[49] M. Arratia, Y. Song, F. Ringer, and B. Jacak, (2019), 1912.05931.

[50] M. Dasgupta, F. Dreyer, G. P. Salam, and G. Soyez, JHEP **04**, 039 (2015), 1411.5182.

[51] T. Kaufmann, A. Mukherjee, and W. Vogelsang, Phys. Rev. D **92**, 054015 (2015), 1506.01415, [Erratum: Phys.Rev.D 101, 079901 (2020)].

[52] Z.-B. Kang, F. Ringer, and I. Vitev, JHEP **10**, 125 (2016), 1606.06732.

[53] L. Dai, C. Kim, and A. K. Leibovich, Phys. Rev. D **94**, 114023 (2016), 1606.07411.

[54] L. Dai, C. Kim, and A. K. Leibovich, Phys. Rev. D **95**, 074003 (2017), 1701.05660.

[55] A. H. Mueller, Phys. Lett. B **104**, 161 (1981).

[56] A. Bassetto, M. Ciafaloni, G. Marchesini, and A. H. Mueller, Nucl. Phys. B **207**, 189 (1982).

[57] Y. Dokshitzer, G. Marchesini, and G. Salam, Phys. Lett. B **634**, 504 (2006), hep-ph/0511302.

[58] C.-H. Kom, A. Vogt, and K. Yeats, JHEP **10**, 033 (2012), 1207.5631.

[59] D. P. Anderle, T. Kaufmann, M. Stratmann, and F. Ringer, Phys. Rev. D **95**, 054003 (2017), 1611.03371.

[60] B. Basso and G. Korchemsky, Nucl. Phys. B **775**, 1 (2007), hep-th/0612247.

[61] Y. Hatta, JHEP **11**, 057 (2008), 0810.0889.

[62] D. Neill and F. Ringer, (2020), 2003.02275.

[63] H.-M. Chang, M. Procura, J. Thaler, and W. J. Waalewijn, Phys. Rev. D **88**, 034030 (2013), 1306.6630.

[64] H.-M. Chang, M. Procura, J. Thaler, and W. J. Waalewijn, Phys. Rev. Lett. **111**, 102002 (2013), 1303.6637.

[65] B. Page, X. Chu, and E. Aschenauer, Phys. Rev. D **101**, 072003 (2020), 1911.00657.

[66] L. Zheng, E. Aschenauer, J. Lee, B.-W. Xiao, and Z.-B. Yin, Phys. Rev. D **98**, 034011 (2018), 1805.05290.

[67] S. Höche and S. Prestel, Eur. Phys. J. **C75**, 461 (2015), 1506.05057.